Multiphoton Ionization and *ab Initio* Calculation Studies of the Hydrogen-Bonded Clusters $C_4H_5N-(H_2O)_n$

Yue Li,* Xiang-Hong Liu, Xiu-Yan Wang, and Nan-Quan Lou

State Key Laboratory of Molecular Reaction Dynamics, Dalian Institute of Chemical Physics, Chinese Academy of Sciences, Dalian 116023, P.R. China

Received: September 21, 1998; In Final Form: December 23, 1998

The multiphoton ionization of the hydrogen-bonded clusters $C_4H_5N-(H_2O)_n$ was studied using a time-of-flight mass spectrometer at the laser wavelengths of 355 and 532 nm. At both wavelengths, a series of $C_4H_5N-(H_2O)_n^+$ and the protonated $C_4H_5N-(H_2O)_nH^+$ were obtained. The two-photon resonance ionization processes at 355 nm make this wavelength produce obviously more abundant ions of pyrrole and the clusters than 532 nm. *Ab initio* calculations show that in the protonated products, the proton prefers to link with the α-C of pyrrole rather than with the N atom. The production of the protonated products requires an intracluster proton transfer reaction. The protonated products obtained at 532 nm are suggested to arise from an intracluster penning ionization or a charge transfer process. The abnormally higher intensities of $C_4H_4N-(H_2O)_n^+$ ($n \geq 1$) than those of $C_4H_4N^+$ are attributed to the stabilization effects of the cluster formation on the dissociation products $C_4H_4N^+$ of the pyrrole molecule.

Introduction

The research of hydrogen-bonded clusters has received a great deal of attention of many theoreticians and experimentalists. It has been found that in the ionization processes (including multiphoton ionization, single-photon ionization, and electron impact ionization etc.) of many hydrogen-bonded clusters, the predominant products were the protonated ones, and sometimes they were nearly the only ones.[1−5] These protonated products are suggested to arise from an intracluster proton transfer reaction accompanying the dissociation processes.[6−11] Proton transfer is a fundamental process in life phenomena.[12−13] The investigation of these cluster systems may give us a chance to deeply understand the mechanism of this process through a relatively simple system. Since clusters exist as isolated, finite systems in the gas phase, they are amenable to study by many of the same techniques that have led to great wealth of information on bimolecular gas phase reactions.[14] It is also possible to observe directly how chemical reactivity changes as a function of stepwise solvation by monitoring the changes in reaction channel versus the cluster size.[15−16] Thus, it can provide the information on the effects of solvents on chemical reactions.

Pyrrole (C_4H_5N) is a compound of five-membered heterocyclic aromatic ring, in which a lone pair of electrons offered by the N atom and the two double bonds form a delocalized big π-bond. Many studies on the clusters of the aromatic ring compounds and some small molecules (such as H_2O) have been performed.[17−18] These aromatic compounds exist widely as constituents of larger biomolecules. For example, pyrrole is a building block of several important biological molecules such as amino acids (tryptophan), nucleotide bases and more. Tubergen *et al.*[19] have reported their microwave spectrum results about the cluster comprising C_4H_5N and H_2O. They suggested that the two monomers form a hydrogen-bonded structure, in which pyrrole acts as a proton donor. Accurate rotational constants as well as ^{14}N nuclear quadrupole coupling constants are also presented for this system. Nagy[20] and Martoprawiro *et al.*[21] have calculated the structure, vibrational frequencies, rotational constants, and dipole moments of the cluster using *ab initio* calculation.

Here we report the experimental results of the cluster using a multiphoton ionization (MPI) time-of-flight mass spectrometer at 355 and 532 nm wavelengths. The experimental results were complemented by *ab initio* calculations.

Experimental Section

All experiments were performed on a time-of-flight (TOF) mass spectrometer. A schematic diagram of the TOF mass spectrometer used in the experiment is shown in Figure 1. Pyrrole- and water-mixed clusters were introduced through a 0.37 mm pulsed nozzle in the ionization region located 10 cm downstream from the nozzle without skimming. The laser beam (Nd:YAG with a pulse width of 10 ns, a maximum output power of about 35 mJ for 532 nm and 9 mJ for 355 nm per pulse), focused by a quartz lens, intersected it. Ions formed by the photoionization were accelerated in a double electrostatic field of 1.0 kV and directed through a 1.2 m long free-field flight tube, which was differentially pumped by one 1500 $L\cdot s^{-1}$ and two 450 $L\cdot s^{-1}$ turbomolecular pumps. The base pressure in the drift region typically raised from 8×10^{-5} Pa to about 1×10^{-5} Pa to about 1×10^{-3} Pa during normal operation, The ions were then detected by a chevron microchannel plate (MCP) detector connected with a fast preamplifier. The mass spectrum was recorded by a 500 MHz transient recorder (EG&G, Model 9846-500) coupled with a microcomputer. The experiments were operated at 5 Hz and TOF spectra typically were accumulated from 1024 pulses.

In the cluster formation, experiments were typically performed with a gas mixture consisting of 1% pyrrole (British Drug Houses Ltd., 99.5%) and 1% water seeded in helium (Dalian Chemical Industry LTD, 99.999%) which were expanded at 3 atm stagnation pressure. All samples were used without further purification.

10.1021/jp983789x CCC: $18.00
Published on Web 03/18/1999

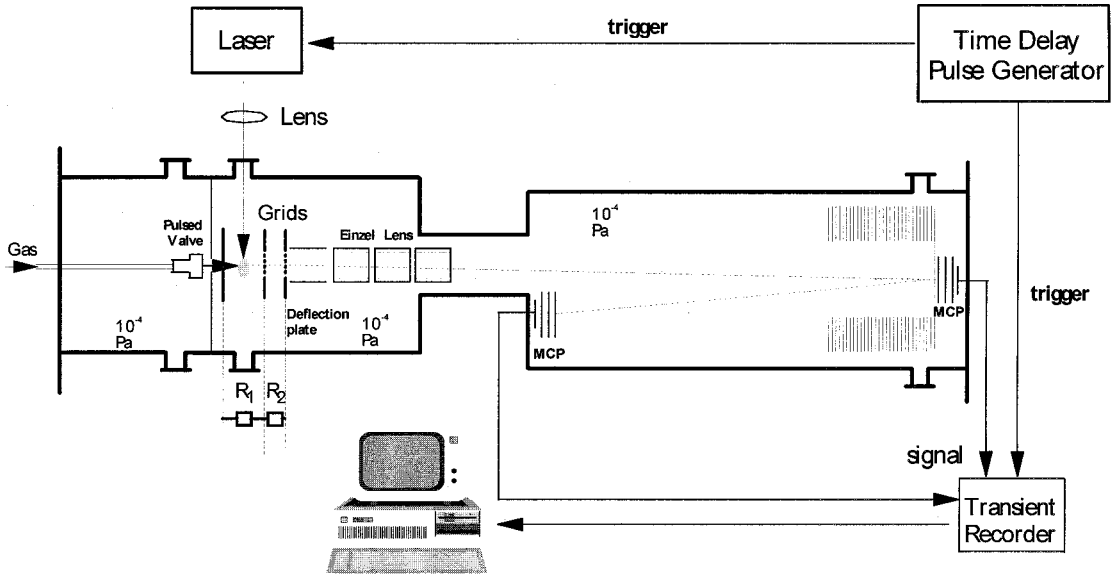

Figure 1. Scheme of the experimental setup.

Computational Methods

For all the molecules and clusters considered in this work, the initial geometries were fully optimized at the unrestricted Hartree−Fock level (UHF) with 6-31G* standard basis set using the analytical gradient techniques. Stationary points and first-order saddle points were confirmed through the calculation of harmonic vibrational frequencies, which were also used to obtain the zero-point energy. The frequencies and zero-point vibrational energies were scaled by 0.893[22] for anharmonicity. For $C_4H_5N-H_2O^+$, the $\langle S^2\rangle$ value was nearly 1.0, which is much higher than the ideal value of 0.75 for a pure doublet state. It indicates the existence of serious spin contamination for the UHF calculation. The UHF method may lead to artificially low relative energies for those isomers having large spin contamination. Thus, the MP4(SDQ)/6-31G* single-point calculations at the UHF/6-31G* optimized geometries were employed to account for electron correlation to obtain more reliable energies. The energies calculated by the spin projected PUMP3 are expected to be more reliable than the regular MP4(SDQ) method for those species with serious spin contamination.[23] Therefore, in the present study, the PUMP3/6-31G*//UHF/6-31G* + 0.893 × ZPE(UHF/6-31G*) method was used to obtain the energies of all species. For the dissociation energy of the neutral $C_4H_5N-H_2O$ cluster, the basis set superposition error (BSSE) correction, which is one of the major factors limiting the accuracy of ab initio calculation of van der Waals interaction in both Hartree−Fock and electron correlation energy calculations, was carried out using the counterpoise (CP) method. To give an estimate about the accuracy of the results obtained at the present calculation level, complete basis set methods (CBS-4)[24] were used to calculate the energies such as the ionization potential and proton affinities of pyrrole. It was known that complete basis set methods can achieve good results for the energy prediction, but the methods are less expensive than G2. All of the above calculations were performed using the Gaussian-94w program package.[25]

Results and Discussion

1. Mass Spectra. The typical multiphoton ionization mass spectra of $C_4H_5N-(H_2O)_n$ clusters at the laser wavelengths of 355 and 532 nm are shown in Figures 2 and 3, respectively. Both figures exhibit a sequence of $C_4H_5N-(H_2O)_n^+$ and

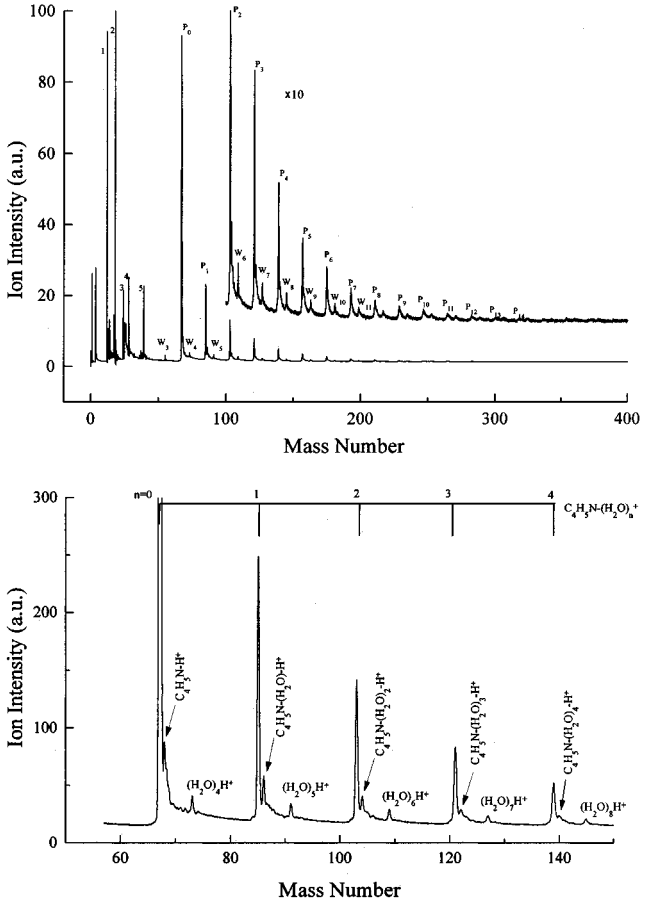

Figure 2. TOF mass spectrum of the pyrrole-water binary clusters obtained at 355 nm: (a) mass number from 0 to 400: (1) C^+ (M = 12), (2) H_2O^+ (M = 18), (3) C_2^+ (M = 24), (4) CH_2N^+ (M = 28), (5) $C_3H_3^+$ (M = 39); P_n, $C_4H_5N-(H_2O)_n^+$; W_n, $(H_2O)_nH^+$; (b) mass number from 60 to 150.

$C_4H_5N-(H_2O)_nH^+$. At 355 nm, the protonated ions $C_4H_5N-(H_2O)_nH^+$ are less abundant than the unprotonated ones, $C_4H_5N-(H_2O)_n^+$. At 532 nm, on the contrary, the protonated clusters have comparable ion intensities as the unprotonated ones. The dissociation products, $C_4H_4N-(H_2O)_n^+$, can be seen at a high laser power at 532 nm, but not at 355 nm. The power of the laser has a considerable effect on multiphoton processes

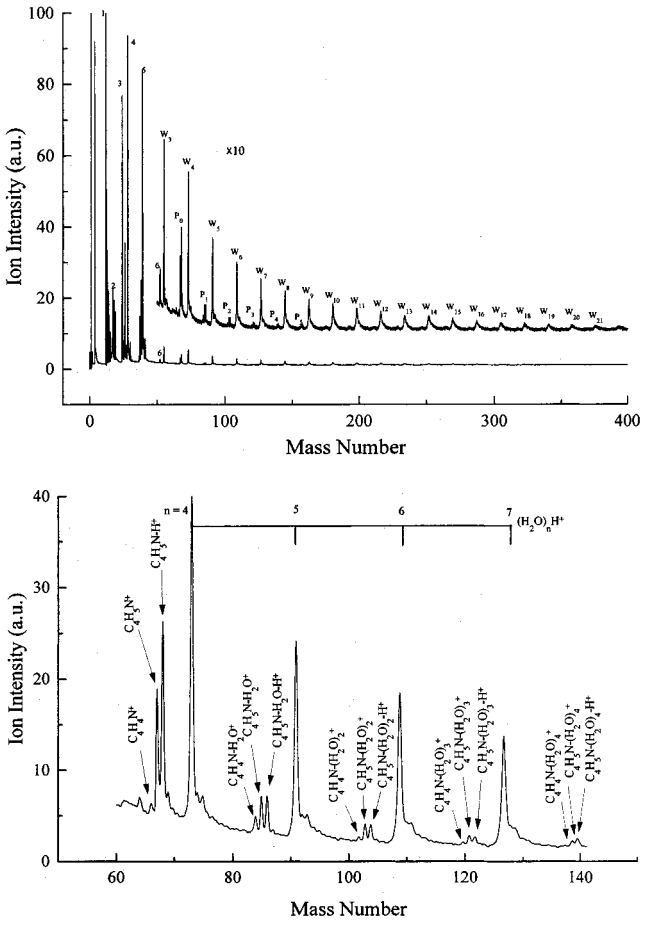

Figure 3. TOF mass spectrum of the pyrrole-water binary clusters obtained at 532 nm: (a) mass number from 0 to 400: (1) C^+ (M = 12), (2) H_2O^+ (M = 18), (3) C_2^+ (M = 24), (4) CH_2N^+ (M = 28), (5) $C_3H_3^+$ (M = 39), $C_4H_4^+$ (M = 52); P_n, $C_4H_5N-(H_2O)_n^+$; W_n, $(H_2O)_nH^+$; (b) mass number from 60 to 150.

inducing ionization and dissociation. The maximum laser power of 532 nm was about 4 times higher than that of 355 nm. Thus, it is expected that pyrrole and the clusters are easier to dissociate at 532 nm than at 355 nm. In Figures 2 and 3, the ion intensities of the two series of clusters decrease with increasing n value and there are not any obvious "magic" numbers to be found. At both wavelengths, a series of protonated water cluster ions $(H_2O)_nH^+$ and photofragments of the pyrrole can also be seen, and the latter indicates that the dissociation of pyrrole occurs upon the ionization of the molecule.

Comparison of Figure 2 with Figure 3 indicates that, at the same conditions of molecular beam and laser power, the ion intensities of the $C_4H_5N-(H_2O)_n^+$ series (including $C_4H_5N^+$) at 532 nm are 1 order of magnitude less than those at 355 nm. The ionization potential of pyrrole (8.21 eV) is lower than that of water (12.6 eV). Although the formation of clusters can make the value a little red-shifted,[26] it may be deduced that the ionization of $C_4H_5N-(H_2O)_n$ needs at least three photons at 355 nm. The dependence of the ion intensities on the laser energy shows that all the power indices of $C_4H_5N^+$ and $C_4H_5N-(H_2O)_n^+$ ($n \geq 1$) approximate to 1.2. It may indicate the following two results: (1) At 355 nm, the ionization mechanism of $C_4H_5N-(H_2O)_n$ may be similar to that of C_4H_5N; namely the ionization processes of the mixed clusters take place mainly on the pyrrole molecule; (2) the fact that the power indices are not integers implies that some dissociation processes have taken place upon the excitation or ionization. This conclusion can be confirmed by intense dissociation fragments measured in the mass spectra. Blank *et al.*[27] have investigated the ultraviolet photodissociation dynamics of the pyrrole molecule by photofragment translational spectroscopy. Several dissociation channels and dissociation energies were also presented. The unimolecular decomposition of ionic pyrrole were also investigated with the photoion−photoelectron coincidence technique and charge-exchange mass spectrometry by Willett[28] and Tedder *et al.*[29] The appearance potentials (AP) of several fragment ions were obtained. Pickett[30] and Bavia *et al.*[31] measured the UV absorption spectra of pyrrole. The electronic spectra of pyrrole have also been studied using multiconfigurational second-order perturbation theory (CASPT2).[32] On the basis of their results, two photons of 355 nm wavelength can excite the pyrrole molecule from the ground state to a vibronic state of the excited state $4^1A_1(2b_1-3p\pi)$ (6.78 eV). Hence, the power index 1.2 may indicate the production of $C_4H_5N-(H_2O)_n^+$, which arises from a near-two-photon resonance process through the 4^1A_1 intermediate state of pyrrole. However, it should be noted that three photons of the 532 nm wavelength can also excite the molecule to the excited state. Although the laser power of 532 nm is higher than that of 355 nm, the probability of a three-photon process should be much less than that of a two-photon process. Therefore, it is displayed that the ion intensities of $C_4H_5N-(H_2O)_n^+$ measured at 355 nm are much higher than at 532 nm.

2. Protonated Clusters $C_4H_5N-(H_2O)_nH^+$. In the above mass spectra, a series of protonated cluster ions $C_4H_5N-(H_2O)_nH^+$ are produced at both wavelengths. They should be the products of the following ionization−intracluster proton transfer−dissociation reactions:

$$C_4H_5N-(H_2O)_m + h\nu \rightarrow C_4H_5N-(H_2O)_m^+ + e^- \rightarrow C_4H_5N-(H_2O)_nH^+ + (H_2O)_{m-n-1} + OH + e^- \quad (1)$$

Figure 4 depicts the calculated equilibrium structures and parameters of both neutral and ionic $C_4H_5N-(H_2O)$ at the UHF/6-31G* level. The energies of pyrrole and the cluster species are also listed in Table 1. Experimental structure parameters are available for the neutral pyrrole in the ground state from its microwave spectrum[33] and theoretical calculations.[34−38] Takeshita and Yamamoto[35] have calculated the molecular structures and the vibrational levels of the low-lying ionic states ($^2A_2$, $^2B_1$, $^2A_1$, and $^2B_2$) of pyrrole. The present results are in agreement with their for C_4H_5N and $C_4H_5N^+$ in the ground state.

For the neutral $C_4H_5N-(H_2O)$ cluster, two initial structures (I and II) were optimized, in which pyrrole and water act as a proton donor, respectively. Figure 4 shows that the neutral (I) has a linear hydrogen-bonded structure, in which C_4H_5N acts as a proton donor and the two H atoms of H_2O are located nearly symmetrically on both sides of the pyrrole plane, which makes the cluster have an approximate symmetry of the C_{2v} point group. The calculations show that the N···H−O hydrogen-bonded structure, in which H_2O acts as a proton donor, does not exist. An unexpected structure (II) was obtained, in which water lies over the ring of pyrrole and its two H atoms point unsymmetrically to the aromatic ring. This structure is considered to be the one in which the π-electron cloud of pyrrole forms two hydrogen bonds with water (as in benzene−water[39]). $C_4H_5N-H_2O$(II) has a higher energy than type I. Thus, it can be deduced that the stable configuration of $C_4H_5N-H_2O$ should be type I. The conclusion is consistent with the experimental and calculational results of Tubergen[19] and Nagy.[20] The hydrogen bond in the pyrrole−water system is predicted to be comparable with, and even a little stronger than, that in the water dimer.

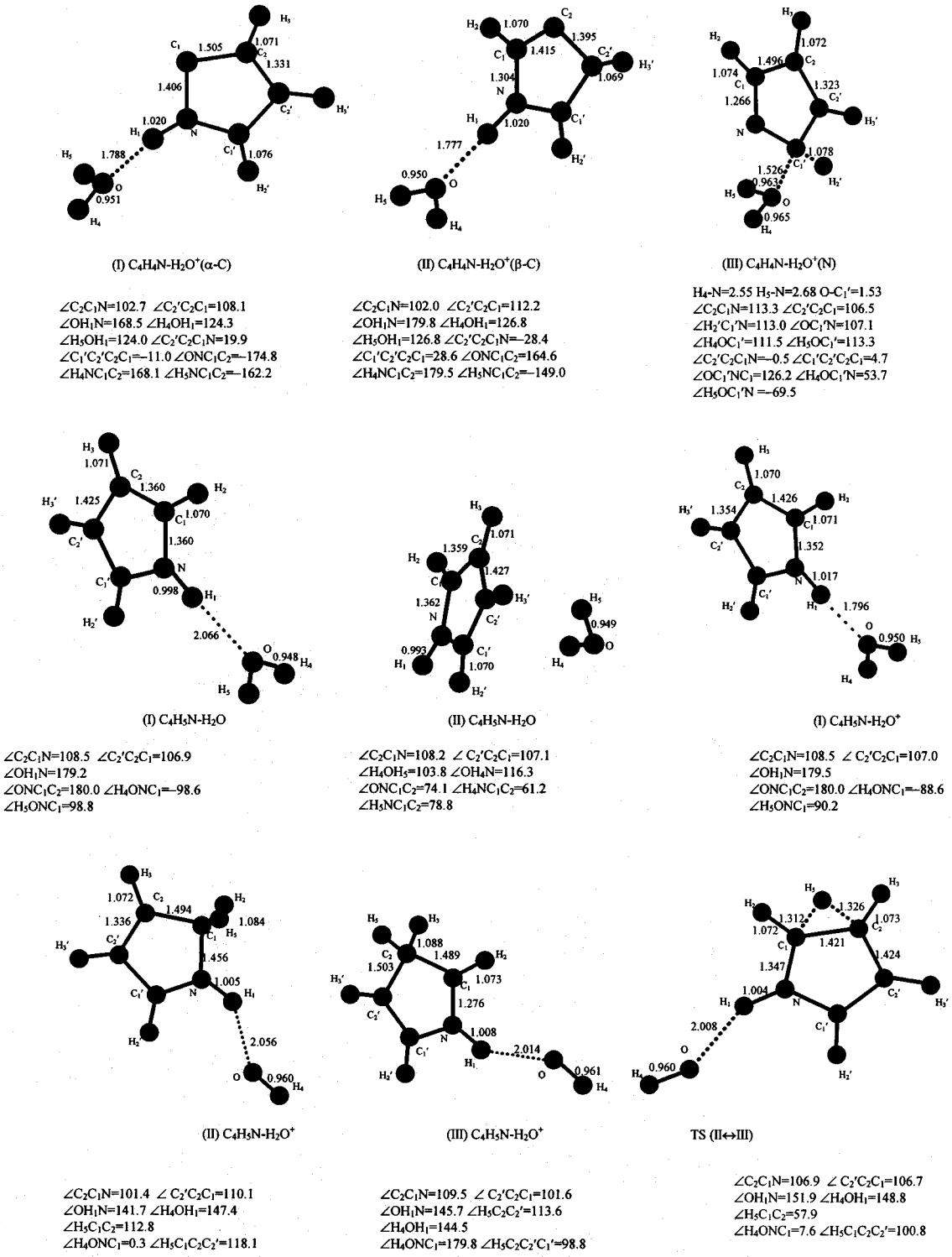

Figure 4. Obtained structures of the pyrrole-water cluster species calculated at the UHF/6-31G* level.

For ionic $C_4H_5N-H_2O^+$, three kinds of conformations were obtained. Type I is similar to the neutral(I), but the N−H bond length of the hydrogen bond increases and the O−H bond length decreases. It indicates that two monomers of the ionic cluster have stronger interactions than the neutral one. Types II and III correspond to the structures in which one H atom of H_2O in type I is transferred onto the α-C and *β*-C atoms of the pyrrole ring, respectively. Their two H atoms on α-C (or *β*-C) are located symmetrically on the two sides of the pyrrole ring. The N, H, and O atoms form a bend angle, where the O−H bond length is obviously longer than that of type I. In the sixth structure in Figure 4, the H_5 atom of TS (the transition state of the transformation from ionic type II to III) has an approximately equal distance from C_1 and C_2. The Mulliken population analysis of ionic $C_4H_5N-(H_2O)^+$ (I) shows that the total atomic charges of the pyrrole and water molecules are 0.956 and 0.044, respectively; i.e., the positive charge is located mainly at the pyrrole molecule. It is in accordance with the fact that pyrrole has a lower ionization energy.

The calculated energy diagram for the $C_4H_5N-H_2O$ binary cluster and the energy changes of reactions for the system are summarized in Figure 5 and Table 2. Table 2 also lists the results

TABLE 1: Calculated Total Energies (*E*) and Zero-Point Energies (ZPE) (hartrees)

species	*E*(HF)[a]	ZPE[a]	*E*(PMP3)[b]	*E*(MP4)[c]
H	−0.4982	0	−0.4982	−0.4982
OH	−75.3823	0.0091	−75.5333	−75.5345
H_2O	−76.0107	0.0230	−76.2020	−76.2046
$C_4H_4N^+$(N)[d]	−207.8927	0.0736	−208.5369	−208.5457
$C_4H_4N^+$(α-C)[d]	−207.8533	0.0741	−208.4989	−208.5090
$C_4H_4N^+$(β-C)[d]	−207.8373	0.0744	−208.5041	−208.5137
C_4H_5N	−208.8079	0.0888	−209.5003	−209.5070
$C_4H_5N^+$	−208.5691	0.0864	−209.2272	−209.2307
$C_4H_5NH^+$(N)[d]	−209.1351	0.1035	−209.8228	−209.8303
$C_4H_5NH^+$(α-C)[d]	−209.1733	0.1026	−209.8533	−209.8618
$C_4H_5NH^+$(β-C)[d]	−209.1615	0.1019	−209.8456	−209.8541
$C_4H_5N-H_2O$(I)	−284.8271	0.1136	−285.7130	−285.7223
$C_4H_5N-H_2O$(II)	−284.8245	0.1138	−285.7103	−285.7195
$C_4H_5N-H_2O^+$(I)	−284.6078	0.1124	−285.4607	−285.4663
$C_4H_5N-H_2O^+$(II)	−284.5726	0.1138	−285.4061	−285.4157
$C_4H_5N-H_2O^+$(III)	−284.5618	0.1119	−285.3992	−285.4063
$C_4H_5N-H_2O^+_{ver}$[e]	−284.5938	0.1124	−285.4451	−285.4522
$C_4H_5N-H_2O-H^+$(N)[d]	−285.1750	0.1290	−286.0578	−286.0678
$C_4H_5N-H_2O-H^+$(α-C)[d]	−285.2106	0.1284	−286.0859	−286.0970
$C_4H_5N-H_2O-H^+$(β-C)[d]	−285.2003	0.1278	−286.0794	−286.0904
$C_4H_4N-H_2O^+$(α-C)[d]	−283.8929	0.1001	−284.7343	−284.7470
$C_4H_4N-H_2O^+$(β-C)[d]	−283.8770	0.1003	−284.7376	−284.7500
$C_4H_4N-H_2O^+$(N)[d]	−283.9529	0.1067	−284.8120	−284.8230
TS(II↔III)	−284.5172	0.1097	−285.3600	−285.3686

[a] UHF/6-31G*//UHF/6-31G* values. [b] PUMP3(SDQ)/6-31G*//UHF/6-31G* values. [c] MP4(SDQ)/6-31G*//UHF/6-31G* values. [d] N, α-C, and β-C in the parentheses represent that the gain or loss of the hydrogen atom (or the proton) occurs on N, α-C, and β-C of pyrrole, respectively. [e] The subscript ver indicates vertical ionization.

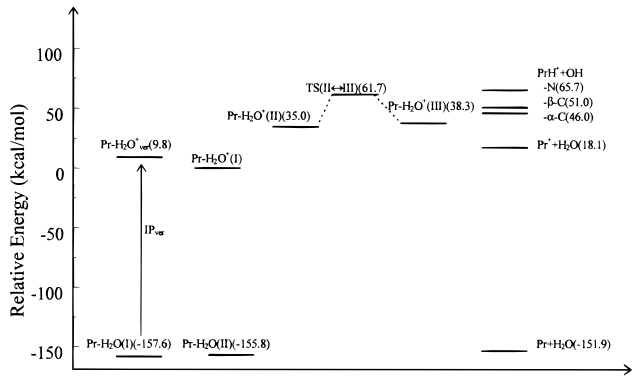

Figure 5. Energy diagram for the dissociation of neutral and ionic $C_4H_5N-H_2O$ clusters. The energies of all species were obtained at the PUMP3(SDQ)/6-31G*//UHF/6-31G* level with zero-point energy corrections. The values in the parentheses represent relative energies and $C_4H_5N-H_2O^+$ (type I) is set to be zero. Pr represents C_4H_5N and the subscript ver indicates vertical ionization.

obtained by complete basis set methods and other techniques for comparison. It can be seen that the calculation results obtained at the present level of theory are in agreement with other available calculational and experimental results, except the ionization potentials of C_4H_5N and $C_4H_5N-H_2O$ were underestimated by about 20 kcal/mol when comparing with the experimental result of Williamson *et al.*[40] and the calculational results of complete basis set methods. Thus, we expect that the results given in Table 2 are of semiquantitative of accuracy.

Table 2 shows that the ionization potential of the $C_4H_5N-H_2O$ cluster is red-shifted by about 12 kcal/mol with respect to that of the C_4H_5N molecule. For protonated pyrrole, three isomers are suggested and they correspond to the structures in which the proton links with the N, α-C, or β-C atoms of the pyrrole ring, respectively. Protonation sites in the heterocycles including the N atom are relevant to their chemical reactivity and biological functioning. Therefore, the protonation of pyrrole has been extensively studied through experiment and theory. In an ion cyclotron resonance study, Houriet *et al.*[41−42] used hydrogen−deuterium exchange between deuterated pyrrole and a reference base to bracket the proton affinities (PA) of pyrrole between 205 and 208 kcal/mol and suggested that protonation occurs at α-C. However, protonation at β-C could not be excluded. In this study, $C_4H_5NH^+$(α-C) has the lowest energy and hence is the most stable protonated isomer. Therefore, α-C was the most basic site. The calculated PA in pyrrole are 194, 214, and 209 kcal/mol for protonation at N, α-C, and β-C, respectively, which are in good agreement with the recent results of Nguyen *et al.*,[43] but is slightly higher than the reported experimental values for pyrrole (208−209 kcal/mol).[44−45]

The structures of the protonated products $C_4H_5N-H_2O-H^+$ were also optimized based on the initial conformations corresponding to those in which the proton links to N, α-C, β-C of pyrrole, and the O atom of H_2O, respectively. The calculations show that the energy of the conformation in which the proton links to α-C is the lowest, which is in agreement with the above results for C_4H_5N. The calculations did not obtain the equilibrium structure in which the proton links to O; thus we think that the structure can not exist stably. Table 2 shows that the PA of $C_4H_5N-H_2O$ for N, α-C, and β-C are 208, 226, and 222 kcal/mol, respectively, and increase by about 12 kcal/mol relative to the pyrrole molecule.

From Figure 5, it can be deduced that when $C_4H_5N-H_2O$ is vertically ionized, unprotonated products $C_4H_5N^+$ and H_2O should be the predominant dissociation products because the channel has the lowest energy. The protonated $C_4H_5NH^+$ should have less abundances with respect to the unprotonated ones. The results are consistent with the experimental results obtained at 355 nm. The above discussions show that the produced protonated cluster ions correspond to the structures whose protons link with the α-C atom of pyrrole, but not the N atom. In consideration of the fact that in the liquid phase reactions, α-C of pyrrole has a very strong activity of electrophilic substitution reactions (the transition state of α-substitution is more stable and the electropositivity of the pyrrole ring can disperse on three atoms (with three resonance structures, as contrasted with the β-substitution which has only two resonance structures[46])), the above conclusion is not unexpected.

The protonated $C_4H_5NH^+$(α-, β-C) correspond to the dissociation products of $C_4H_5N-H_2O^+$(II) and -(III), respectively. Their production requires an intracluster proton transfer process (corresponding to a rearrangement of the ionic structure I → II or III) taking place in advance. Figure 5 shows that the transformation of II ↔ III need get through a transition state TS and must overcome an energy barrier of about 30 kcal/mol.

3. Mechanism of Formation of the Protonated Cluster Ions $C_4H_5N-(H_2O)_nH^+$ at 532 nm. From Figure 3, it can be seen that at 532 nm, $C_4H_5N-(H_2O)_nH^+$ have comparable intensities with $C_4H_5N-(H_2O)_n^+$ and the abundance of $C_4H_5NH^+$ is even higher than that of $C_4H_5N^+$. It was found in the experiments that at 532 nm, the variance patterns of the $C_4H_5N-(H_2O)_n^+$ ion intensities with the laser power were different from those of $C_4H_5N-(H_2O)_nH^+$. Figure 6 provides the ion intensities variance of $C_4H_5N^+$, $C_4H_5NH^+$, and H_2O versus laser power. It shows that the protonated products are more dependent on the laser power than the unprotonated ones. At 532 nm, the ionization of pyrrole and water needs at least 4 and 6 photons, respectively. The power indices of $C_4H_5N^+$, $C_4H_5NH^+$, and H_2O^+ measured in the experiments are approximately 1.4, 2.5, and 3.0, respectively. The facts imply that the formation mechanism of $C_4H_5N^+$ is different from that of $C_4H_5NH^+$. The

TABLE 2: Summary of the Reaction Energy Changes for Pyrrole and the Pyrrole−Water Binary Cluster System[a]

		reaction	energy (kcal/mol)	other results (kcal/mol)
1	C_4H_5N	$\rightarrow C_4H_5N^+$	IP = 170.1	173.6,[c] 189.2,[d] 175.4,[d] 189.1,[e] 190.5[f]
2	$C_4H_5N^+$	$\rightarrow C_4H_4N^+ + H$	D_0 = 113.3	122.5,[f] 107.0[g]
3		$\rightarrow C_4H_4N^+(\alpha\text{-C}) + H$	D_0 = 137.4	
4		$\rightarrow C_4H_4N^+(\beta\text{-C}) + H$	D_0 = 134.3	
5	$C_4H_5N + H^+$	$\rightarrow C_4H_5NH^+(N)$	PA = 194.1	186.7,[f] 188[h]
6		$\rightarrow C_4H_5NH^+(\alpha\text{-C})$	PA = 213.7	204.4,[f] 207,[h] 208−209[i,j] 205−208[k]
7		$\rightarrow C_4H_5NH^+(\beta\text{-C})$	PA = 209.3	200.0,[f] 202[h]
8	$C_4H_5N-H_2O$(I)	$\rightarrow C_4H_5N-H_2O^+$(I)	IP = 157.6	180.3[f]
9		$\rightarrow C_4H_5N-H_2O^+{}_{ver}$[b]	IP_{ver} = 167.4	
10		$\rightarrow C_4H_5N + H_2O$	D_0 = 4.4	6.78[l]
11	$C_4H_5N-H_2O$(II)	$\rightarrow C_4H_5N + H_2O$	D_0 = 2.1	5.63[l]
12	$C_4H_5N-H_2O^+$(I)	$\rightarrow C_4H_5N^+ + H_2O$	D_0 = 18.1	
13		$\rightarrow C_4H_5NH(N)^+ + OH$	D_0 = 65.7	
14		$\rightarrow C_4H_5NH(\alpha\text{-C})^+ + OH$	D_0 = 46.0	
15		$\rightarrow C_4H_5NH(\beta\text{-C})^+ + OH$	D_0 = 51.0	
16	$C_4H_5N-H_2O^+$(II)	$\rightarrow C_4H_5NH(\alpha\text{-C})^+ + OH$	D_0 = 11.0	
17	$C_4H_5N-H_2O^+$(III)	$\rightarrow C_4H_5NH(\beta\text{-C})^+ + OH$	D_0 = 12.7	
18	$C_4H_5N-H_2O^+$(II)	$\rightarrow$ TS(II↔III)	ΔE = 26.7	
19	$C_4H_5N-H_2O^+$(III)	$\rightarrow$ TS(II↔III)	ΔE = 23.4	
20	$C_4H_5N-H_2O^+$(I)	$\rightarrow C_4H_4N-H_2O(\alpha\text{-C})^+ + H$	D_0 = 136.2	
21		$\rightarrow C_4H_4N-H_2O(\beta\text{-C})^+ + H$	D_0 = 134.3	
22		$\rightarrow C_4H_4N-H_2O(N)^+ + H$	D_0 = 91.2	
23	$C_4H_5N-H_2O$(I) + H^+	$\rightarrow C_4H_5N-H_2O-H^+(N)$	PA = 207.6	
24		$\rightarrow C_4H_5N-H_2O-H^+$(a-C)	PA = 225.6	
25		$\rightarrow C_4H_5N-H_2O-H^+(\beta\text{-C})$	PA = 221.9	

[a] PUMP3(SDQ)/6-31G*//UHF/6-31G* values (with zero-point energy correction). [b] The subscript ver indicates vertical ionization. [c] Reference 33. [d] Reference 35. [e] Reference 38. [f] CBS-4 values. [g] $D_0(N-H) = AP(C_4H_4N^+) - IP(C_4H_5N)$. [h] Reference 41. [i] Reference 42. [j] Reference 43. [k] Reference 40. [l] Reference 20.

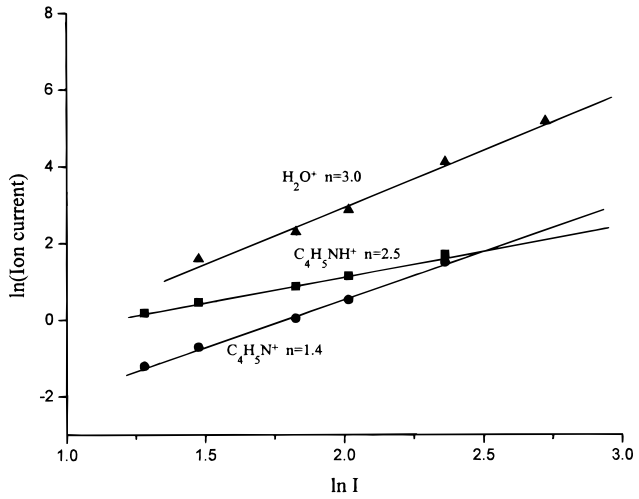

Figure 6. Schematic illustration of the ion intensity variance of $C_4H_5N^+$, $C_4H_5NH^+$, and H_2O^+ versus laser power.

unprotonated pyrrole cluster ions should arise from the following reactions:

$$C_4H_5N-(H_2O)_m + kh\nu \rightarrow C_4H_5N^+-(H_2O)_m + e^-$$
(the pyrrole molecule is ionized)

$$\rightarrow C_4H_5N-(H_2O)_n^+ + (H_2O)_{m-n} + e^- \quad \text{(major process)} \quad (2)$$

the following process may also occur:

$$C_4H_5N^+-(H_2O)_m \rightarrow C_4H_5N-(H_2O)_nH^+ + (H_2O)_{m-n-1} + OH \quad \text{(minor process)} \quad (3)$$

i.e., the ionization process takes place on the pyrrole molecule in the mixed clusters, and the predominant products of the dissociation are the unprotonated ones. The stronger dependence on the laser power of the protonated products indicates that their production relates to the excitation or ionization of water. The following intracluster penning ionization or charge transfer processes are suggested:

$$C_4H_5N-(H_2O)_m + kh\nu \rightarrow C_4H_5N-(H_2O)_m{}^*$$
(the H_2O molecule is excited)

$$\rightarrow C_4H_5N^+-(H_2O)^{\ddagger} + e^-$$
(intracluster penning ionization)

$$\rightarrow C_4H_5N-(H_2O)_nH^+ + (H_2O)_{m-n-1} + OH + e^-$$
(major process)

$$\rightarrow C_4H_5N-(H_2O)_n^+ + (H_2O)_{m-n} + e^- \quad \text{(minor process)} \quad (4)$$

$$C_4H_5N-(H_2O)_m + kh\nu \rightarrow C_4H_5N-(H_2O)_m{}^+ + e^-$$
(the H_2O molecule is ionized)

$$\rightarrow C_4H_5N^+-(H_2O)_m{}^{\ddagger} + e^- \quad \text{(intracluster charge transfer)}$$

$$\rightarrow C_4H_5N-(H_2O)_nH^+ + (H_2O)_{m-n-1} + OH + e^-$$
(major process)

$$\rightarrow C_4H_5N-(H_2O)_n^+ + (H_2O)_{m-n} + e^- \quad \text{(minor process)} \quad (5)$$

where the * means electronic excited state and ‡ indicates vibrational excited state.

Shafizadeh[47] and Atkins[48] *et al.* studied the photodissociation of H_2O through two-photon resonance excitation of the B^1A_1 state using 266 nm wavelength laser. The resonance energy also corresponds to the four-photon energy of 532 nm wavelength. The energy is higher than the ionization potential of the pyrrole

monomer. Thus, the production of $C_4H_5NH^+$ may relate to a four-photon resonance excitation process of the H_2O molecule. After that, an intracluster Penning ionization or ionization-charge transfer process follows, and the excess energy is released into the vibrational modes of the clusters that causes the clusters to be dissociated. The obtained products correspond to the protonated ones whose production, as shown in the above calculations, needs higher energies than the unprotonated ones. Garvey *et al.*[49] have studied the ionization of argon/methanol mixed clusters using electron impact. They found that appearance potentials of $Ar_n(CH_3OH)_m$ fall in the region of 11.3−11.8 eV and suggested that the threshold ionization of the clusters is mediated by the Ar 4s excited states; i.e., an intracluster Penning ionization plays a role on the ionization of the clusters. In the photoionization of van der Waals cluster ArHCl,[50] an intracluster charge transfer and vibrational predissociation mechanism is also presented to interpret the obvious decrease of the photoionization cross sections of ArHCl than the expected. Thus, this kind of intracluster penning ionization and charge transfer processes often occur in the ionization of heterogeneous clusters with weak interactions, in which different molecular subunits can be selectively excited or ionized.[50] These processes influence the photoionization and photodissociation mechanisms of the clusters.

The formation of clusters can increase effectively ionization cross sections of monomers.[50] Thus, the participation of $(H_2O)_n$ in the ionization of the cluster species which is followed by the intracluster Penning ionization, charge transfer, and vibrational predissociation processes may be a reason why the intensities of $C_4H_5NH^+$ are even higher than those of $C_4H_5N^+$.

4. Formation of the Photofragments $C_4H_4N-(H_2O)_n^+$. Figure 3 shows a sequence of photofragments of $C_4H_4N-(H_2O)_n^+$. These photofragments are thought to be produced through the following dissociation reactions:

$$C_4H_5N-(H_2O)_m + kh\nu \rightarrow C_4H_4N-(H_2O)_n^+ + (H_2O)_{m-n} + H + e^- \ (n \geq 0) \quad (6)$$

Table 2 shows that for $C_4H_5N^+$, the dehydrogenation reaction occurs most easily by removing the H atom from the N atom because $C_4H_4N^+$(N) has the lowest energy. The unimolecular decomposition of pyrrole has been investigated using photoion−photoelectron coincidence technique.[28] The measured AP of $C_4H_4N^+$ is 12.85eV (296.2 kcal/mol). Using the IP value of pyrrole and the equation $D_0(N-H) = AP(C_4H_4N^+) - IP(C_4H_5N)$, the $D_0(N-H)$ is deduced to be 107.0 kcal/mol, which is consistent with the value 113 kcal/mol here suggested.

Figure 3 shows that with respect to $C_4H_5N-(H_2O)_n^+$ ($n \geq 1$), the abundances of $C_4H_4N-(H_2O)_n^+$ ($n \geq 1$) cluster ions are even a little higher than those of $C_4H_4N^+$ relative to $C_4H_5N^+$. In the photodissociation of the clusters, the H atom linking with N forms a hydrogen bond with H_2O, which makes its loss difficult due to cage effect.[51] Thus, for $C_4H_4N-H_2O^+$, only three initial equilibrium structures were optimized, in which the H atoms on α-C, β-C of pyrrole, and H_2O are lost, respectively. As shown in Figure 4, $C_4H_4N-(H_2O)^+$ (α-C or β-C) is similar to a complex of $C_4H_4N^+$ (α-C or β-C) and H_2O. For the initial structure corresponding to losing H of H_2O, the calculations give $C_4H_4N-H_2O^+$ (III), in which the distances between H_4, H_5, and O are 0.965 and 0.963 Å, but H_4, H_5, and N have the distances of 2.549 and 2.683 Å, respectively. Therefore, this structure should not be looked as a complex comprising $C_4H_5N^+$ and OH, $C_4H_5N-OH^+$, but a complex comprising $C_4H_4N^+$(N) and H_2O, $C_4H_4N-H_2O^+$(N); namely, for $C_4H_5N-H_2O^+$, the loss of H still occurs on the N atom of pyrrole, and H of H_2O is not easy to be lost. The distance between C_1' and O is 1.526 Å in $C_4H_4N-H_2O^+$(N) and it indicates that a C−O bond has been formed.

For dissociation products of $C_4H_5N-H_2O^+$, the calculations show that $C_4H_4N-H_2O^+$(N) has the lowest energy. The necessary energy of its production is 91.2 kcal/mol, which is smaller by nearly 20 kcal/mol than that of $C_4H_4N^+$(N). Namely, the formation of clusters reduces the necessary energy for the dissociation of $C_4H_5N-H_2O^+$. The reduction of the dissociation energy can be thought to arise from the stabilization effects of the cluster formation on the dissociation products $C_4H_4N^+$ of the pyrrole molecule. It is to be explanation of why the abundances of the sequence of $C_4H_4N-(H_2O)_n^+$ ($n \geq 1$) are even higher than those of $C_4H_4N^+$.

It is interesting to consider that when the clusters are ionized and excited, the dissociation fragments are not the products of the break of the relative weaker bond between pyrrole and water, but the O−H of water or the C−H bond of pyrrole. In a series of experiments, Stace *et al.*[52−54] have made extensive studies of unimolecular decomposition of molecular ions (such as methanol) in association with inert gas (e.g., Ar and CO_2) clusters using electron impact. In their study, the heterocluster ions $Ar_nCH_xO^+$ ($x = 0-4$) were observed. Stace interpreted these results in terms of an intracluster charge exchange ionization between argon and methanol. A model was also proposed incorporating competition between the unimolecular decomposition of the methanol component and dissipation of the molecular vibrational energy into the van der Wasls modes of the cluster, which in turn lead to loss of argon from the cluster via vibrational predissociation. For most of weak interaction molecules studied so far, the vibrational predissociation times should be considerably shorter than the time scales of any of the alternative deexcitation routes.[53] However, if an excited van der Waals or hydrogen-bonded clusters consists of a polyatomic molecule with a low density of vibrational states at the excitation energy complexed with other atoms or molecules, intramolecular vibrational relaxation (IVR) may influence events by introducing a time lag between excitation and vibrational predissociation. Vibrational energy present in the excited mode may not flow directly to that mode which is most strongly coupled to the van der Waals bond or the hydrogen bond. This could have the effect of reducing the vibrational predissociation time to a value where it would be comparable with other slower processes, such as fluorescence and unimolecular decay. Under such circumstance, two or more of the deexcitation channels could operate in competition and the relative time scale for vibrational predissociation could actually be longer than that for covalent bond fission. Thus, for the $C_4H_5N-(H_2O)_n$ cluster system, the fragmentation of the N−H bond or the C−H bond of pyrrole, but not the hydrogen bond between pyrrole and water, is possible.

Conclusion

The multiphoton ionization of the hydrogen-bonded clusters $C_4H_5N-(H_2O)_n$ was studied with a time-of-flight mass spectrometer at the laser wavelengths of 355 and 532 nm. The results show that, at both wavelenghts, a series of $C_4H_5N-(H_2O)_n^+$ and $C_4H_5N-(H_2O)_nH^+$ were obtained. The near-two-photon resonance ionization processes through the $4^1A_1(2b_1-3p\pi)$ intermediate state at 355 nm make this wavelength produce obviously more abundant ions of pyrrole and the clusters than 532 nm. *Ab initio* calculations show that in the protonated products, the proton prefers to link with the α-C, β-C atoms

rather than the N atom. The production of the protonated products requires an intracluster proton transfer process induced by laser. The protonated products obtained at 532 nm are suggested to arise from an intracluster Penning ionization or charge transfer process following the excitation or ionization of water. The abnormal intensities of $C_4H_4N-(H_2O)_n^+$ ($n \geq 1$) are attributed to the stabilization effects of the cluster formation on the dissociation products $C_4H_4N^+$ of the pyrrole molecule.

References and Notes

(1) Choo, K. Y.; Shinohara, H.; Nishi, N. *Chem. Phys. Lett.* **1983**, *95*, 102.

(2) Shinohara, H.; Nagashima, U.; Nishi, N. *Chem. Phys. Lett.* **1984**, *111*, 511.

(3) Xia, P.; Garvey, J. F. *J. Phys. Chem.* **1995**, *99*, 3448.

(4) Xia, P.; Hall, M.; Furlani, T. R.; Garvey, J. F. *J. Phys. Chem.* **1996**, *100*, 12235.

(5) Lee, S. Y.; Shin, D. N.; Cho, S. G.; Jung, K. H. *J. Mass Spectrom.* **1995**, *30*, 969.

(6) Gellene, G. I.; Porter, R. F.; *J. Phys. Chem.* **1984**, *88*, 6680.

(7) Misaizu, F.; Houston, P. L.; Nishi, N.; Shinohara, H.; Kondow, T.; Kinoshita, M. *J. Phys. Chem.* **1989**, *93*, 7041.

(8) Wei, S.; Purnell, J.; Buzza, S. A.; Stanley, R. J.; Castleman, A. W., Jr. *J. Chem. Phys.* **1992**, *97*, 9480.

(9) Wei, S.; Purnell, J.; Buzza, S. A.; Stanley, R. J.; Castleman, A. W., Jr. *J. Chem. Phys.* **1993**, *99*, 755.

(10) Castleman, A. W., Jr.; Wei, S. *Annu. Rev. Phys. Chem.* **1994**, *45*, 685.

(11) Bernstein, E. R. *Annu. Rev. Phys. Chem.* **1995**, *46*, 197.

(12) Caldin, E., Gold, V., Eds. *Proton Transfer Reactions*; Wiley, New York, 1975, and references cited therein.

(13) Mitchell, P. *Annu. Rev. Biochem.* **1977**, *46*, 996.

(14) Kebarle, P. *Annu. Rev. Phys. Chem.* **1977**, *28*, 445.

(15) Hineman, M. F.; Kelley, D. F.; Bernstein, E. R. *J. Chem. Phys.* **1993**, *99*, 4533.

(16) Droz, T.; Knochenmuss, R.; Leutwyler, S. *J. Chem. Phys.* **1990**, *93*, 4320.

(17) Feller, D.; Feyereisen, M. W. *J. Comput. Chem.* **1993**, *14*, 1027.

(18) Sun, S.; Bernstein, E. R. *J. Phys. Chem.* **1996**, *100*, 13348.

(19) Tubergen, M. J.; Andrews, A. M.; Kuczkowski, R. L. *J. Phys. Chem.* **1993**, *97*, 7451.

(20) Nagy, P. I.; Durant, G. J.; Smith, D. A. *J. Am. Chem. Soc.* **1993**, *115*, 2912.

(21) Martoprawiro, M. A.; Bacskay, G. B. *Mol. Phys.* **1995**, *85*, 573.

(22) Pople, J. A.; Gordon, M. H.; Fox, D. J.; Raghavachari, K.; Curtiss, L. A. *J. Chem. Phys.* **1989**, *90*, 5622.

(23) Huang, J. H.; Han, K. L.; Deng, W. Q.; He, G. Z. *Chem. Phys. Lett.* **1997**, *273*, 205.

(24) Ochterski, J. W.; Petersson, G. A. *J. Chem. Phys.* **1996**, *104*, 2598.

(25) Frisch, M. J.; Trucks, G. W.; Gordon, M. H.; Gill, P. M. W.; Wong, M. W.; Foresman, J. B.; Johnson, B. G.; Schlegel, H. B.; Robb, M. A.; Replogle, E. S.; Gomperts, R.; Andres, J. L.; Raghavachari, K.; Binkley, J. S.; Gonzales, C.; Martin, R. L.; Fox, D. J.; Defrees, D. J.; Baker, J.; Stewart, J. J. P.; Pople, J. A. *GAUSSIAN 94W* (Revision A), Gaussian, Inc.: Pittsburgh, PA, 1995.

(26) Li, Y.; Liu, X. H.; Wang, X. Y.; Lou, N. Q. *Chem. Phys. Lett.* **1997**, *276*, 339.

(27) Blank, D. A.; North, S. W.; Lee, Y. T. *Chem. Phys.* **1994**, *187*, 35.

(28) Willett, G. D.; Baer, T. *J. Am. Chem. Soc.* **1980**, *102*, 6774.

(29) Tedder, J. M.; Vidaud, P. H. *J. Chem. Soc., Faraday Trans. 2* **1980**, *76*, 1523.

(30) Pickett, L. W.; Corning, M. E.; Wieder, G. M.; Semenov, D. A.; Buckley, J. M. *J. Am. Chem. Soc.* **1953**, *75*, 1618.

(31) Bavia, M.; Bertinelli, F.; Taliani, C.; Zauli, C. *Mol. Phys.* **1976**, *31*, 479.

(32) Andres, L. S.; Merchan, M.; Gil, I. N.; Roos, B. O.; Fulscher, M. *J. Am. Chem. Soc.* **1993**, *115*, 6184.

(33) Nygaard, L.; Nielsen, J. T.; Kirchheiner, J.; Maltesen, G.; Rastrup-Andersen, J.; Sorensen, G. O. *J. Mol. Struct.* **1969**, *3*, 491.

(34) Kofranek, M.; Kovar, T.; Karpfen, A.; Lischka, H. *J. Chem. Phys.* **1992**, *96*, 4464.

(35) Takeshita, K.; Yamamoto, Y. *J. Chem. Phys.* **1994**, *101*, 2198.

(36) Lee, S. Y.; Boo, B. H. *J. Phys. Chem.* **1996**, *100*, 15073.

(37) Nyulaszi, L.; Veszpremi, T. *Int. J. Quant. Chem.* **1997**, *61*, 399.

(38) Jiang, J. C.; Tsai, M. H. *J. Phys. Chem.* **1997**, *101*, 1982.

(39) Gotch, A. J.; Zwier, T. S. *J. Chem. Phys.* **1992**, *96*, 3388.

(40) Williamson, A. D.; Compton, R. N.; Eland, J. H. D. *J. Chem. Phys.* **1979**, *70*, 590.

(41) Houriet, R.; Schwarz, H. *Lect. Notes Chem.* **1982**, *31*, 229.

(42) Houriet, R.; Schwarz, H.; Zummack, W.; Andrade, J. G.; Schleyer, P. V. R. *New J. Chem.* **1981**, *5*, 505.

(43) Nguyen, V. Q.; Turecek, F. *J. Mass Spectrom.* **1996**, *31*, 1173.

(44) Szulejko, J. E.; McMahon, T. B. *J. Am. Chem. Soc.* **1993**, *115*, 7839.

(45) Lias, S. G.; Bartmess, J. E.; Liebman, J. F.; Holmes, J. L.; Levin, R. D.; Mallard, G. W. *J. Phys. Chem. Ref. Data* **1988**, *17*, Suppl. 1.

(46) Xu, J. G. *The Gound of Organic Chemistry*; Advanced Education Press of China: Beijing, 1986.

(47) Shafizadeh, N.; Rostas, J.; Lemaire, J. L.; Rostas, F. *Chem. Phys. Lett.* **1988**, *152*, 75.

(48) Atkins, C. G.; Briggs, R. G.; Halpern, J. B.; Hancock, G. *Chem. Phys. Lett.* **1988**, *152*, 81.

(49) Vaidyanathan, G.; Coolbaugh, M. T.; Peifer, W. R.; Garvey, J. F. *J. Chem. Phys.* **1991**, *94*, 1850.

(50) Li, Y.; Wang, X. Y.; Zhang, X. G.; Li, L. B.; Lou, N. Q.; Sheng, L. S.; Zhang, Y. W. *Chem. Phys. Lett.* **1997**, *278*, 63.

(51) Gerber, R. B.; MeCoy, A. B.; Garcia-Vela, A. *Annu. Rev. Phys. Chem.* **1994**, *45*, 275.

(52) Stace, A. J. *J. Phys. Chem.* **1987**, *91*, 1509.

(53) Stace, A. J. *J. Am. Chem. Soc.* **1985**, *107*, 755.

(54) Bernard, D. M.; Gotts, N. G.; Stace, A. J. *Int. J. Mass Spectrom. Ion Processes* **1990**, *95*, 327.